



# *N,N'*-bis(5-bromo-2-hydroxy-3-methoxybenzylidene)-1,3-diaminopropane Cu–4f–Cu and Cu–4f complexes: Synthesis, crystal structures and magnetic properties

Beata Cristóvão<sup>a,\*</sup>, Barbara Mirosław<sup>b</sup>, Julia Kłak<sup>c</sup>

<sup>a</sup> Department of General and Coordination Chemistry, Maria Curie-Skłodowska University, Maria Curie-Skłodowska sq. 2, 20-031 Lublin, Poland

<sup>b</sup> Department of Crystallography, Faculty of Chemistry, Maria Curie-Skłodowska University, Maria Curie-Skłodowska sq. 3, 20-031 Lublin, Poland

<sup>c</sup> Faculty of Chemistry, University of Wrocław, F. Joliot Curie 14, 50-383 Wrocław, Poland

## ARTICLE INFO

### Article history:

Received 25 July 2011

Accepted 15 December 2011

Available online 23 December 2011

### Keywords:

Heterotrinnuclear complexes

Heterodinuclear complexes

Schiff base

Crystal structure

Magnetic properties

## ABSTRACT

Synthesis, crystal structures and magnetic studies of new heterotri- and heterodinuclear complexes having general formulae  $[\text{Cu}_2\text{Ln}(\text{L})_2(\text{NO}_3)(\text{H}_2\text{O})_2](\text{NO}_3)_2 \cdot 3\text{H}_2\text{O}$  (where Ln = Ce (**1**), Pr (**2**), Nd (**3**) and La (**4**)), and  $[\text{CuLn}(\text{L})(\text{NO}_3)_2(\text{H}_2\text{O})_3\text{MeOH}]\text{NO}_3 \cdot \text{MeOH}$  (where Ln = Dy (**5**) and Er (**6**)), respectively involving the Schiff base ( $\text{H}_2\text{L}$ ) as main ligand are reported. The heterotrinnuclear complexes crystallize in the monoclinic space group  $C2/c$  with the molecule lying on the twofold axis ( $Z' = 0.5$ ), while the dinuclear complexes (**5** and **6**) form monoclinic crystals with space group  $P2_1/n$ . The lanthanide(III) cation in  $\text{Cu}^{\text{II}}-\text{Ln}^{\text{III}}-\text{Cu}^{\text{II}}$  core is 10-coordinated, whereas in dinuclear compounds the coordination number for Ln(III) ion is only nine. The polyhedra formed around terminal Cu(II) ions in **1–3** have a shape of deformed tetragonal pyramid with water molecule in apical position. In crystals **5** and **6** the Cu(II) has octahedral coordination. The temperature dependence of the magnetic susceptibility and the field-dependent magnetization indicated that the interaction between  $\text{Cu}^{\text{II}}$  and  $\text{Ln}^{\text{III}}$  ions is antiferromagnetic for Ln = Ce, Pr and Nd and ferromagnetic for Ln = Dy and Er.

© 2011 Elsevier Ltd. All rights reserved.

## 1. Introduction

Schiff base ligands obtained from salicylaldehyde and its derivatives are largely used for the synthesis of metal complexes having application in bioinorganic chemistry, catalysis and magnetochemistry [1–7]. The molecular structure of these ligands – the kind, the number and the position of the donor atoms influence the number of metal ions within homo- and heteronuclear compounds [1,5,8–12]. Additional coordinating groups (for example: methoxy) attached to salicylaldehyde yield compartmental Schiff base ligands which have an inner coordination site with two N-donor and two O-donor chelating centers suitable for the complexation of transition metal ions, and outer coordination site with four O-donor atoms that is capable of incorporating larger oxophilic ions, such as rare earth elements [5,9–11,13–18]. The Ln(III) ions (except for La, Gd and Lu) have a large orbital contribution to the total magnetic moment, which makes the understanding of the 3d–4f interaction complicated [6,13,19–25]. In the reported 3d–4f compounds, where the nature or magnitude of the interactions has been determined, the majority of them contain Gd(III) as the lanthanide counterpart [6,9–11,15–17,26–29]. Kahn et al.

predicted theoretically that coupling of  $4f^n$  ions with other paramagnetic species will be antiferromagnetic for  $n < 7$  and ferromagnetic for  $n > 7$  [30,31].

The studies of the crystal structure and magnetic interaction in di- and polynuclear metal 3d–4f complexes are crucial in the development of the coordination chemistry and magnetochemistry. As a continuation of our research in the present paper we report synthesis, molecular and crystal structures (except **4**) and magnetic properties of four novel heterotrinnuclear  $[\text{Cu}_2\text{Ce}(\text{L})_2(\text{NO}_3)(\text{H}_2\text{O})_2](\text{NO}_3)_2 \cdot 3\text{H}_2\text{O}$  (**1**),  $[\text{Cu}_2\text{Pr}(\text{L})_2(\text{NO}_3)(\text{H}_2\text{O})_2](\text{NO}_3)_2 \cdot 3\text{H}_2\text{O}$  (**2**),  $[\text{Cu}_2\text{Nd}(\text{L})_2(\text{NO}_3)(\text{H}_2\text{O})_2](\text{NO}_3)_2 \cdot 3\text{H}_2\text{O}$  (**3**) and  $[\text{Cu}_2\text{La}(\text{L})_2(\text{NO}_3)(\text{H}_2\text{O})_2](\text{NO}_3)_2 \cdot 3\text{H}_2\text{O}$  (**4**) and two heterodinuclear  $[\text{CuDy}(\text{L})(\text{NO}_3)_2(\text{H}_2\text{O})_3\text{MeOH}]\text{NO}_3 \cdot \text{MeOH}$  (**5**) and  $[\text{CuEr}(\text{L})(\text{NO}_3)_2(\text{H}_2\text{O})_3\text{MeOH}]\text{NO}_3 \cdot \text{MeOH}$  (**6**) compounds with the Schiff base ligand *N,N'*-bis(5-bromo-3-methoxysalicylidene)propylene-1,3-diamine ( $\text{H}_2\text{L}$ , Scheme 1).

## 2. Experimental

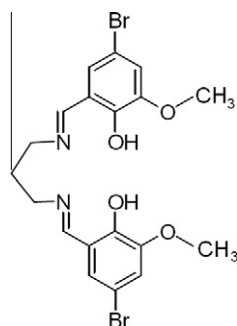
### 2.1. Synthesis

#### 2.1.1. Materials

The reagents and solvents used for synthesis were commercially available from Aldrich Chemical Company and Polish Chemical Reagents. They were used as received without further purification.

\* Corresponding author.

E-mail address: [beata.cristovao@poczta.umcs.lublin.pl](mailto:beata.cristovao@poczta.umcs.lublin.pl) (B. Cristóvão).



Scheme 1. Structure of ligand molecule  $H_2L$ .

### 2.1.2. $N,N'$ -bis(5-bromo-3-methoxysalicylidene)propylene-1,3-diamine, $H_2L$

The Schiff base ( $C_{19}H_{18}Br_2N_2O_4$ ) abbreviated as  $H_2L$  was obtained by the 2:1 condensation of 5-bromo-2-hydroxy-3-methoxybenzaldehyde and 1,3-diaminopropane in methanol according to the reported procedure [11,12,17]. *Anal. Calc.* for  $C_{19}H_{18}Br_2N_2O_4$ : C, 45.61; H, 4.00; N, 5.60. *Found:* C, 45.37; H, 3.84; N, 5.57%. FTIR (KBr,  $cm^{-1}$ ): 34520w, 1636s, 1574w, 1476s, 1440w, 1392w, 1252s, 1096m, 1068m, 1016w, 968m, 864m, 852m, 836m, 756m.  $^1H$  NMR (DMSO- $d_6$ ,  $\delta$  ppm):  $-CH=N-$ , 8.50; Ar-OH, 13.78; H-Ar, 7.10, 7.20 (doublet AB);  $-OCH_3$ , 3.79;  $-CH_2-N-$ , 3.68 (triplet);  $-CH_2-$ , 2.03 (quintet).

### 2.1.3. $[Cu_2Ln(L)_2(NO_3)(H_2O)_2](NO_3)_2 \cdot 3H_2O$ , ( $Ln = Ce$ **1**, Pr **2**, Nd **3**, La **4**) and $[CuLn(L)(NO_3)_2(H_2O)_3MeOH]NO_3 \cdot MeOH$ ( $Ln = Dy$ **5**, Er **6**)

The **1–6** complexes were prepared according the same experimental procedure, so that only the cerium(III) entity (**1**) will be described. The Schiff base ligand  $H_2L$  (0.4 mmol, 0.1999 g) was dissolved in methanol (20 mL) at room temperature. Then copper(II) acetate monohydrate (0.4 mmol, 0.0799 g) followed by cerium(III) nitrate hexahydrate (0.2 mmol, 0.0868 g) were added to the yellow homogeneous solution which was stirred, yielding a clear green solution. The solution was filtered and kept undisturbed during a few days at low temperature in the fridge until green crystals were formed. They were isolated by filtration, washed with cold methanol and air-dried. We have failed to obtain well-shaped single crystals of the lanthanum(III) complex **4** but we have succeeded in doing so for the cerium(III) **1**, praseodymium(III) **2** and neodymium(III) **3** complexes, that turned out to be isostructural. It is worth to note that using the same 3d/4f ratio and synthesis conditions we have obtained different products: trinuclear complexes in the case of light lanthanides(III) **1–4** and dinuclear ones in the case of heavy lanthanides(III) **5, 6**.

*Yield:* 180 mg/59%. *Anal. Calc.* for  $C_{38}H_{46}N_7O_{22}Br_4Cu_2Ce$  (**1**) (1539.66): C, 29.64; H, 2.99; N, 6.37; Cu, 8.25; Ce, 9.10. *Found:* C, 29.76; H, 2.79; N, 6.34; Cu, 8.10; Ce, 8.72%. Selected FTIR bands (KBr,  $cm^{-1}$ ): 3444m, 1624s, 1552w, 1468s, 1384s, 1292s, 1240s, 1220m, 1068w, 788m, 756w, 692w, 628w, 448w.

### 2.1.4. $[Cu_2Pr(L)_2(NO_3)(H_2O)_2](NO_3)_2 \cdot 3H_2O$ (**2**)

*Yield:* 190 mg/62%. *Anal. Calc.* for  $C_{38}H_{46}N_7O_{22}Br_4Cu_2Pr$  (1540.45) (**2**): C, 29.62; H, 2.99; N, 6.37; Cu, 8.25; Pr, 9.15. *Found:* C, 30.04; H, 2.85; N, 6.24; Cu, 8.02; Pr, 9.40%. Selected FTIR bands (KBr,  $cm^{-1}$ ): 3440m, 1628s, 1468s, 1384s, 1288s, 1238m, 1220m, 1076w, 788m, 756w, 692w, 628w, 448w.

### 2.1.5. $[Cu_2Nd(L)_2(NO_3)(H_2O)_2](NO_3)_2 \cdot 3H_2O$ (**3**)

*Yield:* 170 mg/55%. *Anal. Calc.* for  $C_{38}H_{46}N_7O_{22}Br_4Cu_2Nd$  (1543.78) (**3**): C, 29.57; H, 2.98; N, 6.35; Cu, 8.24; Nd, 9.34. *Found:* C, 29.86; H, 2.86; N, 6.30; Cu, 8.22; Nd, 9.27%. Selected FTIR bands

(KBr,  $cm^{-1}$ ): 3420m, 1628s, 1560w, 1468s, 1384s, 1288s, 1236m, 1220m, 1076w, 788m, 756w, 692w, 628w, 448w.

### 2.1.6. $[Cu_2La(L)_2(NO_3)(H_2O)_2](NO_3)_2 \cdot 3H_2O$ (**4**)

*Yield:* 180 mg/58%. *Anal. Calc.* for  $C_{38}H_{46}N_7O_{22}Br_4Cu_2La$  (1538.05) (**4**): C, 29.67; H, 2.99; N, 6.38; Cu, 8.26; La, 9.03. *Found:* C, 28.96; H, 3.03; N, 6.25; Cu, 8.32; La, 8.81%. Selected FTIR bands (KBr,  $cm^{-1}$ ): 3440m, 1624s, 1552w, 1468s, 1384s, 1296s, 1240s, 1220m, 1100w, 1068m, 1028w, 848w, 788m, 756w, 692m, 628w, 568w, 468w.

### 2.1.7. $[CuDy(L)(NO_3)_2(H_2O)_3MeOH]NO_3 \cdot MeOH$ (**5**)

*Yield:* 105 mg/52%. *Anal. Calc.* for  $C_{21}H_{32}N_5O_{18}Br_2CuDy$  (1028.38) (**5**): C, 24.50; H, 3.11; N, 6.81; Cu, 6.17; Dy, 15.80. *Found:* C, 25.75; H, 2.92; N, 6.84; Cu, 6.32; Dy, 15.48%. Selected FTIR bands (KBr,  $cm^{-1}$ ): 3426m, 2928w, 2848w, 1628vs, 1560w, 1476s, 1384s, 1240s, 1096m, 1072m, 1012w, 966w, 852w, 820w, 792m, 762m, 696w, 572m, 540w, 448m.

### 2.1.8. $[CuEr(L)(NO_3)_2(H_2O)_3MeOH]NO_3 \cdot MeOH$ (**6**)

*Yield:* 110 mg/55%. *Anal. Calc.* for  $C_{21}H_{32}N_5O_{18}Br_2CuEr$  (1033.14) (**6**): C, 24.39; H, 3.10; N, 6.76; Cu, 6.16; Er, 16.35. *Found:* C, 25.75; H, 2.57; N, 6.20; Cu, 6.33; Er, 15.17%. Selected FTIR bands (KBr,  $cm^{-1}$ ): 3426m, 2928w, 2848w, 1628vs, 1560w, 1476s, 1384s, 1240s, 1096m, 1072m, 1012w, 966w, 852w, 820w, 792m, 762m, 696w, 572m, 540w, 448m.

## 2.2. Methods

The contents of carbon, hydrogen and nitrogen in the analyzed compounds were determined by elemental analysis using a CHN 2400 Perkin Elmer analyser.

The contents of copper and lanthanides were established using ED XRF spectrophotometer (Canberra-Packard).

The  $^1H$  NMR spectra of the Schiff base ligand was recorded in DMSO- $d_6$  solution using Bruker Avance spectrometer (range 0–16  $\delta$  ppm).

The FTIR spectra of complexes were recorded over the range of 4000–400  $cm^{-1}$  using M-80 spectrophotometer (Carl Zeiss Jena). Samples for FTIR spectra measurements were prepared as KBr discs.

The magnetization of the  $Cu^{II}-Ce^{III}-Cu^{II}$  (**1**),  $Cu^{II}-Pr^{III}-Cu^{II}$  (**2**),  $Cu^{II}-Nd^{III}-Cu^{II}$  (**3**),  $Cu^{II}-La^{III}-Cu^{II}$  (**4**),  $Cu^{II}-Dy^{III}$  (**5**) and  $Cu^{II}-Er^{III}$  (**6**) powdered samples was measured over the temperature range of 1.8–300 K using a Quantum Design SQUID – based MPMSXL-5-type magnetometer. The superconducting magnet was generally operated at a field strength ranging from 0 to 5 T. Measurements were made at magnetic field 0.5 T. The SQUID magnetometer was calibrated with the palladium rod sample. Corrections are based on subtracting the sample – holder signal and contribution  $\chi_D$  estimated from the Pascal's constants [32].

## 2.3. X-ray crystal structure determination

The X-ray diffracted intensities were measured from single crystals on an Oxford Diffraction Xcalibur CCD diffractometer with the graphite-monochromatized  $MoK\alpha$  radiation ( $\lambda = 0.71073$  Å) at 100(2) K for **1** and **3** and on an Oxford Diffraction Xcalibur Atlas Gemini ultra diffractometer with monochromatized  $CuK\alpha$  radiation ( $\lambda = 1.54184$  Å) at 293(2) K for **2, 5** and **6**. Data sets were collected using the  $\omega$  scan technique. The programs CRYSLIS CCD and CRYSLIS RED [33] were used for data collection, cell refinement and data reduction. A multi-scan absorption correction was applied for **1** and **3**, while for **2, 5** and **6** – the analytical absorption correction based on the indexing of the crystal faces was performed [34]. The structures were solved by direct methods using SHELXS-97 and

**Table 1**  
Crystallographic data for crystals **1–3** and **5–6**.

	<b>1</b>	<b>2</b>	<b>3</b>	<b>5</b>	<b>6</b>
Empirical formula	C <sub>38</sub> H <sub>46</sub> Br <sub>4</sub> Cu <sub>2</sub> N <sub>7</sub> O <sub>22</sub> Ce	C <sub>38</sub> H <sub>46</sub> Br <sub>4</sub> Cu <sub>2</sub> N <sub>7</sub> O <sub>22</sub> Pr	C <sub>38</sub> H <sub>46</sub> Br <sub>4</sub> Cu <sub>2</sub> N <sub>7</sub> O <sub>22</sub> Nd	C <sub>21</sub> H <sub>32</sub> Br <sub>2</sub> CuN <sub>5</sub> O <sub>18</sub> Dy	C <sub>21</sub> H <sub>32</sub> Br <sub>2</sub> CuN <sub>5</sub> O <sub>18</sub> Er
Formula weight	1539.66	1540.45	1543.78	1028.38	1033.14
T (K)	100(2)	293(2)	100(2)	293(2)	293(2)
Crystal system	monoclinic	monoclinic	monoclinic	monoclinic	monoclinic
Space group	C2/c	C2/c	C2/c	P2 <sub>1</sub> /n	P2 <sub>1</sub> /n
a (Å)	16.841(1)	16.958(1)	16.884(1)	9.952(1)	9.936(1)
b (Å)	13.805(1)	14.082(1)	13.700(1)	16.826(1)	16.808(1)
c (Å)	21.683(1)	21.788(1)	21.720(1)	20.178(1)	20.159(1)
β (°)	93.72(1)	93.99(1)	94.10(1)	90.62(1)	90.71(1)
V (Å <sup>3</sup> )	5030.2(2)	5190.3(2)	5011.1(6)	3378.6(1)	3366.3(2)
Z, Z'	4, 0.5	4, 0.5	4, 0.5	4, 1	4, 1
Crystal form/color	block/green	block/green	block/green	block/green	block/green
Crystal size (mm)	0.30 × 0.20 × 0.16	0.48 × 0.20 × 0.18	0.38 × 0.24 × 0.20	0.41 × 0.20 × 0.12	0.40 × 0.35 × 0.20
D <sub>calc</sub> (g cm <sup>-3</sup> )	2.033	1.971	2.046	2.022	2.039
μ (mm <sup>-1</sup> )	4.992	12.383	5.139	15.985	8.795
Absorption correction	multi-scan	analytical	multi-scan	analytical	analytical
θ Range (°)	3.47–27.48	4.07–67.12	2.62–27.48	3.42–67.22	3.42–67.17
Reflections collected/unique (R <sub>int</sub> )	19474/5745 (0.0386)	47926/4629 (0.0396)	18790/5718 (0.0555)	37080/6030 (0.0400)	236595/6011 (0.0586)
Data/parameters	5745/339	4629/344	5718/341	6030/442	6011/439
Goodness-of-fit (GOF) on F <sup>2</sup>	1.520	1.067	1.283	1.028	1.103
R <sub>1</sub> , wR <sub>2</sub> [I > 2σ(I)]	0.0440, 0.0861	0.0285, 0.0774	0.0564, 0.1310	0.0299, 0.0734	0.0291, 0.0733
R <sub>1</sub> , wR <sub>2</sub> (all data)	0.0567, 0.0874	0.0294, 0.0781	0.0731, 0.1351	0.0320, 0.0751	0.0298, 0.0737
Extinction coefficient					
Δρ <sub>max</sub> , Δρ <sub>min</sub> (e Å <sup>-3</sup> )	1.415, -1.503	0.637, -0.635	2.267, -1.079	1.164, -1.288	1.202, -1.15

refined by the full-matrix least-squares on  $F^2$  using the SHELXL-97 [35] (both operating under WinGX [36]). Non-hydrogen atoms with except of disordered C and O atoms were refined with anisotropic displacement parameters.

The C9 atoms of the propyl bridge in all structures are disordered over two positions with sof's for the major part being 0.75(1), 0.61(1), 0.61(2), 0.54(1) and 0.52(1) in **1–3**, **5** and **6**, respectively. In the asymmetric units of **1** and **3** in the outer sphere of complex there are 1.5 water molecules. In **1** one H<sub>2</sub>O molecule is disordered over two positions with sof's 0.65 and 0.35. The second water (sof = 0.5) is disordered over two positions by the twofold axis. In **3** in the outer sphere 1.5 water molecules occupy two positions with sof's 0.75. Hydrogen atoms of water molecules in the inner coordination sphere were found in the difference Fourier map. The water molecules in the outer sphere are disordered and their H atoms were not found. All remaining H-atoms were positioned geometrically and allowed to ride on their parent atoms, with  $U_{iso}(H) = 1.2/1.5 U_{eq}(C \text{ and } O)$ . A summary of the conditions for the data collection and the crystal structure refinement parameters are given in Table 1. The molecular plots were drawn with ORTEP3 for Windows [37], Mercury [38] and Diamond [39].

### 3. Results and discussion

#### 3.1. Description of crystal and molecular structure of the complexes **1–3** and **5–6**

The trinuclear complexes [Cu<sub>2</sub>Ln(L)<sub>2</sub>(NO<sub>3</sub>)(H<sub>2</sub>O)<sub>2</sub>](NO<sub>3</sub>)<sub>2</sub>·3H<sub>2</sub>O (where Ln = Ce (**1**), Pr (**2**) and Nd (**3**), L = C<sub>19</sub>H<sub>18</sub>N<sub>2</sub>O<sub>4</sub>Br<sub>2</sub>) of **1–3** are isostructural and crystallize in the monoclinic space group C2/c. Their schematic diagram is given in Fig. 1a. The crystal structure with atom numbering scheme of **1** is shown in Fig. 1b (atom numbering scheme is analogs for compounds **2** and **3**). Details of the relevant data collection and refinement are summarized in Table 1. The selected bond lengths and angles are given in Table 2. The complexes of **1–3** are isostructural and crystallize in the monoclinic space group C2/c. These compounds are heterotrimeric nuclear monomers built up around a twofold axis that passes through the Ln<sup>III</sup> cation and bisects the nitrate ligand so only half of molecule is symmetrically independent, Z' = 0.5. One distinctive feature

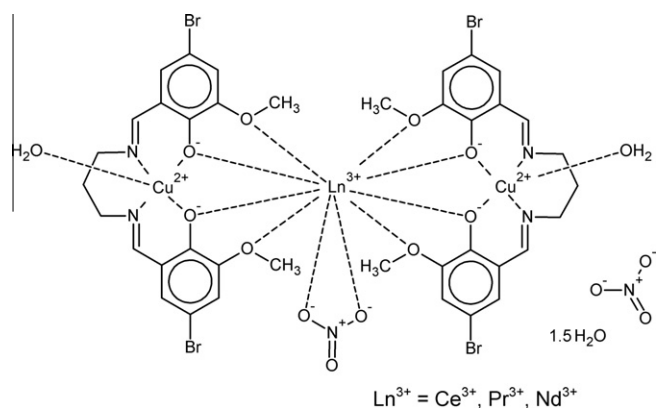


**Fig. 1a.** Schematic diagram of trinuclear complexes **1–3**.

is that the complexes are dicationic [(LCu(H<sub>2</sub>O))<sub>2</sub>Ln(NO<sub>3</sub>)<sub>2</sub>]<sup>2+</sup> and the charge is neutralized by two nitrate ions in the outer coordination sphere. The crystal structures are hydrates with three water molecules (1.5 per asymmetric unit) disordered in channels along Z crystallographic axis (Fig. 2).

The Cu<sup>II</sup> ions occupy the N<sub>2</sub>O<sub>2</sub> cavity. The coordination polyhedron has classical distorted square pyramidal geometry with water molecule in the apical position (Fig. 3). The dihedral angles between two N<sub>2</sub>O<sub>2</sub> planes of the Schiff-base ligands are close to 30° (Table 2). Two O<sub>4</sub> cavities of Schiff base ligands form kind of capsule for the Ln ion. The coordination sphere of the cation is filled by the bidentate (η<sup>2</sup>-chelating) nitrate group. Ten ligand O atoms around the Ln(III) ion form polyhedron in shape of three face- and one edge-capped trigonal bipyramid (Figs. 4). The dihedral angles (α) between the (O1Cu1O2) and (O1Ln1O2) planes are ca. 17° (Table 2). The complexes form chiral two-blade propeller-like left- and right-handed Cu<sup>II</sup>Ln<sup>III</sup>Cu<sup>II</sup> units as in structures reported by Wang et al. [14]. However, the crystals are racemates.

The intramolecular separations Cu<sup>II</sup>⋯Ln<sup>III</sup> and Cu<sup>II</sup>⋯Cu<sup>II</sup> (symmetry code (i) -x + 1, y, -z + 1/2) being ca. 3.6 and 7.2 Å, respectively (Table 2), are within the normal range of values for polynuclear Cu–Ln complexes [9,26].

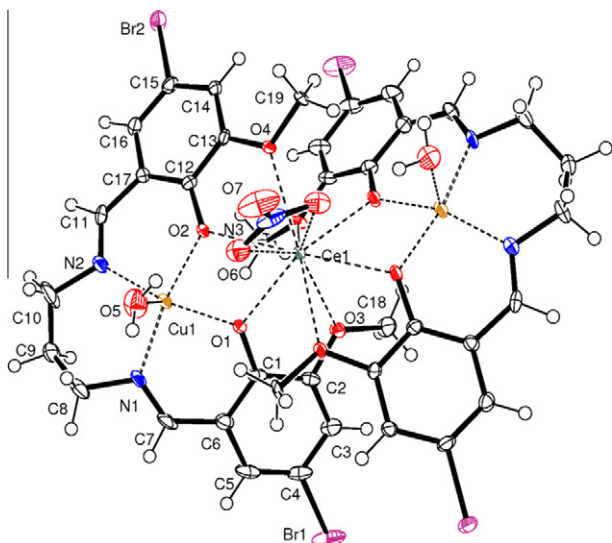


**Fig. 1b.** Molecular structure and atom numbering scheme of complex **1**, displacement ellipsoids were drawn at 50% probability level, hydrogen spheres are drawn with an arbitrary radius; the disordered part of propylene bridge, water molecules and nitrate anion from the outer coordination sphere were omitted for clarity.

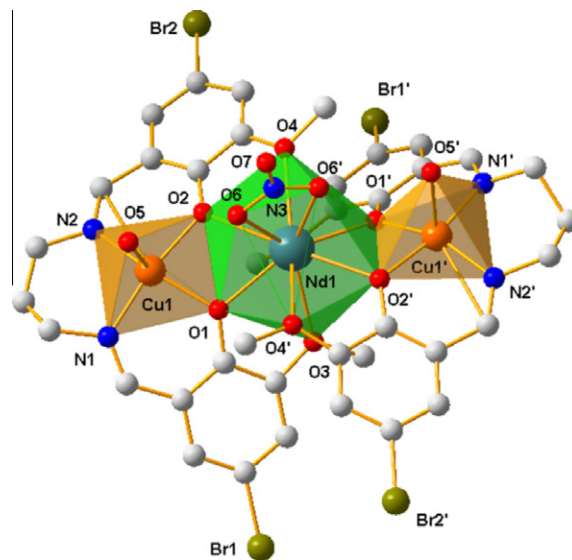


**Fig. 3.** Coordination polyhedra of Cu and Nd cations in the trinuclear complex **3**.

distorted octahedral. The  $\text{Cu}^{2+}$  ion is held within the inner  $\text{N}_2\text{O}_2$  compartment of the Schiff base ligand. The apical vertices of the deformed octahedron are occupied by one methanol and one nitrate oxygen atoms. The dihedral angle between  $\text{Cu1O1O2}$  and  $\text{Ln1O1O2}$  (where  $\text{Ln1} = \text{Dy}, \text{Er}$ ) is equal to  $2.9(1)^\circ$  **5** and  $2.8(1)^\circ$  **6**, respectively that is in accordance with the values reported for similar compounds [11]. The  $\text{Cu1-O}$  and  $\text{Cu1-N}$  bond distances in the equatorial  $\text{N}_2\text{O}_2$  square plane of copper cation for **5** and **6** are very similar and lie in the ranges  $1.949(2)$ – $1.983(2)$  and  $1.959(3)$ – $1.986(3)$  Å, respectively, while in the apical position the  $\text{Cu1-O}$  bond distances are longer (Table 3). The lanthanide–oxygen bond lengths depend on the chemical nature of the O atoms (methoxy, nitrate, aqua or phenoxo). They vary from  $2.323(3)$  Å for  $\text{Er1-O8(aqua)}$  to  $2.524(2)$  Å for  $\text{Dy1-O3(methoxy)}$  (Table 3). The  $\text{Ln-O(phenolate)}$  average bond distance decrease in order of lanthanide radius contraction:  $\text{Gd}$  ( $2.392(5)$  Å) [11] >  $\text{Tb}$  ( $2.375(2)$  Å) [11] >  $\text{Dy}$  ( $2.367(2)$  Å) >  $\text{Er}$  ( $2.345(5)$  Å).

### 3.2. Magnetic properties

The magnetic properties of the heterotrinnuclear complexes,  $\text{Cu}^{\text{II}}\text{-Ce}^{\text{III}}\text{-Cu}^{\text{II}}$  (**1**),  $\text{Cu}^{\text{II}}\text{-Pr}^{\text{III}}\text{-Cu}^{\text{II}}$  (**2**) and  $\text{Cu}^{\text{II}}\text{-Nd}^{\text{III}}\text{-Cu}^{\text{II}}$  (**3**) were determined over the temperature range of 1.8–300 K. Plots of magnetic susceptibility  $\chi_m^{-1}$  and  $\chi_m T$  product versus  $T$  are given in Fig. 5. The experimental  $\chi_m T$  values at room temperature ( $1.54$  for **1**,  $2.24$  for **2** and  $2.23 \text{ cm}^3 \text{ K mol}^{-1}$  for **3**) approximately correspond to the calculated ones  $\chi_m T = ((N\beta^2/3k) [2g_{\text{Cu}}^2 S_{\text{Cu}}(S_{\text{Cu}} + 1) + g_{\text{Ln}}^2 J_{\text{Ln}}(J_{\text{Ln}} + 1)])$  for uncoupled metal ions ( $1.55$ ,  $2.35$  and  $2.38 \text{ cm}^3 \text{ K mol}^{-1}$ , respectively). The  $\chi_m T$  decreases by lowering the temperature to  $0.519$  for **1**,  $0.406$  for **2** and  $0.249 \text{ cm}^3 \text{ K mol}^{-1}$  for **3** in 1.8 K. This decrease could be caused by crystal field effect, as well as cooperative antiferromagnetic interactions of  $\text{Cu}^{\text{II}}\text{-Ln}^{\text{III}}$  pairs. The susceptibility data obey the Curie–Weiss law. Negative value of Weiss constants could also confirm the weak antiferromagnetic exchange coupling between the metal ions ( $-6.8$  K for **1**,  $-9.3$  K for **2** and  $-18.7$  K for **3**). These results are consistent with the empirical studies concerning heterometallic 3d–4f compounds, in which the 4f ions display a spin–orbit coupling [18,19,30,31,40–45]. A final conclusion on the nature of the exchange interaction in compounds cannot be drawn, since the magnetic properties of this type of systems are not only due to the coupling between the 3d and 4f metal ions, but also to the thermal depopulation of the Stark sublevels of the 4f ions.

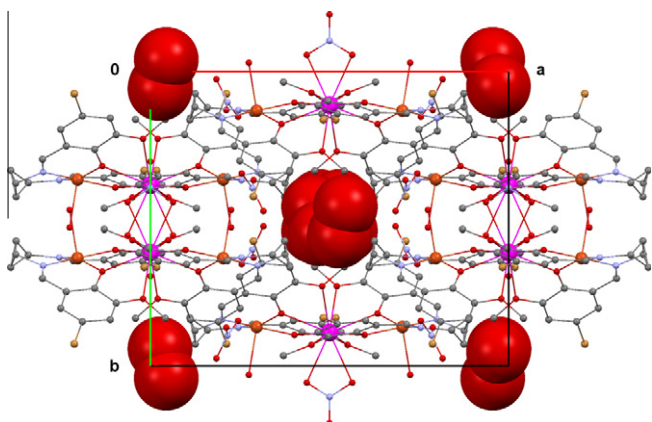


**Fig. 2.** View along channels with disordered water molecules formed in crystal **1**. Hydrogen atoms were omitted for clarity.

The  $\text{Ln-O}$  bond lengths depend on the nature of the oxygen atoms. The distances increase in sequence phenolato < nitrate < methoxo (from  $2.405(4)$  to  $2.636(3)$  Å).

Two  $\text{Cu(II)}$  and one  $\text{Ln(III)}$  ions are arranged nearly in a line, with a  $\text{Cu1-Ln1-Cu1}^{\text{II}}$  (symmetry code (ii):  $1/2 - x, 1/2 + y, 1/2 - z$ ) angles close to  $172^\circ$  (Table 2). Between nitrate ions and water molecules forms extensive network of hydrogen bonds. Intermolecular  $\text{M} \cdots \text{M}$  separations in the  $\text{Cu}^{\text{II}}\text{Ln}^{\text{III}}\text{Cu}^{\text{II}}$  structures indicate well separation of the trinuclear 3d–4f–3d cores (Table 2).

The heterodinuclear complexes  $[\text{CuLn(L)(NO}_3)_2(\text{H}_2\text{O})_3\text{MeOH}]\text{NO}_3 \cdot \text{MeOH}$  (where  $\text{Ln} = \text{Dy}$  (**5**) and  $\text{Er}$  (**6**)) are isostructural with  $\text{Cu}^{\text{II}}\text{-Gd}^{\text{III}}$  and  $\text{Cu}^{\text{II}}\text{-Tb}^{\text{III}}$  coordination compounds reported by us earlier [11] (space group  $P2_1/n$ ). Their schematic diagram is given in Fig. 4a. The crystal structure with atom numbering scheme of **5** is shown in Fig. 4b (atom numbering scheme is analogous for compound **6**). The crystallographic data and experimental details are summarized in Table 1. The selected bond distance and angle values for structures are presented in Table 3. The lanthanide(III) cations in **5** and **6** are nine-coordinated by one bidentate nitrate ion, three water oxygen atoms and four oxygen atoms of the Schiff base. The coordination environment around the copper(II) site is

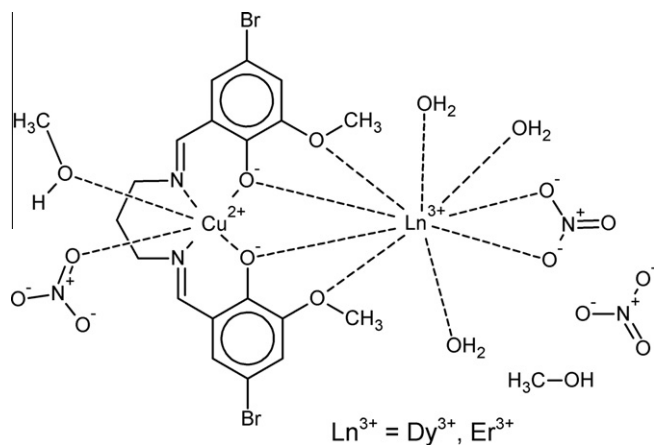


Fig. 4a. Schematic diagram of dinuclear complexes **5** and **6**.

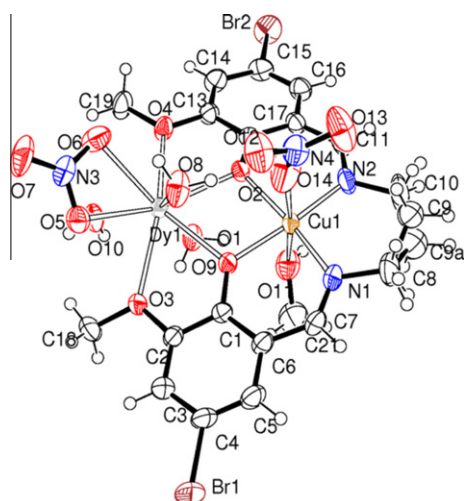


Fig. 4b. Molecular structure and atom numbering scheme of complex **5**, displacement ellipsoids were drawn at 50% probability level, hydrogen spheres are drawn with an arbitrary radius; the methanol molecule and nitrate anion from the outer coordination sphere were omitted for clarity.

To confirm the nature of the ground state of **1**, **2** and **3**, we investigated the variation of the magnetization,  $M$ , with respect to the field, at 2 K. The results are shown in Fig. 6, where molar

magnetization  $M$  is expressed in  $\mu_B$  units. The compounds do not reach the saturation in the applied field range and magnetization in 5 T is equal only to  $1.95 \mu_B$  for **1**,  $1.82 \mu_B$  for **2** and  $1.16 \mu_B$  for **3**. These values are much lower than the simulated values calculated with the Brillouin function for two Cu(II) ions and one Ln(III) ion, which do not interact. This further indicates that all complexes behave as an antiferromagnet. Unfortunately, the quantitative description of the magnetic properties of heterometallic complexes containing lanthanide(III) ions is not an easy task because of the ligand-field effect and spin-orbit coupling of the Ln(III) ion [19,31].

The magnetic susceptibility of Cu<sup>II</sup>–La<sup>III</sup>–Cu<sup>II</sup> (**4**) has been also measured in the temperature range of 1.8–300 K in a 0.5 T applied magnetic field. The data obtained for complex are represented in Fig. 7. At the room temperature, the  $\chi_m T$  product is equal to  $0.884 \text{ cm}^3 \text{ mol}^{-1} \text{ K}$  and it is consistent with only two  $S = 1/2$  copper(II) centers. Lanthanum(III) with an  $^1S_0$  single-ion ground state is diamagnetic. In this compound, the intramolecular Cu...Cu distance is certainly large and may preclude any significant magnetic interactions between the copper centers in trinuclear complex. However, below 10 K, small but discernable drop in the  $\chi_m T$  values to  $0.711 \text{ cm}^3 \text{ K mol}^{-1}$  at 1.8 K was also noted. The thermal dependence of  $\chi_m T$  characteristic of a small antiferromagnetic interaction since no maximum appears in the  $\chi_m$  versus  $T$  curve until 1.8 K. This apparent weak antiferromagnetic interaction may be mediated by the diamagnetic La(III) center. The examples in the literature [26] show, that the diamagnetic lanthanum(III) center are capable of mediating magnetic exchange between the copper(II) in trinuclear complexes.

The magnetization curve for **4** measured at 2 K was reproduced with the Brillouin function for two centers of  $S_{\text{Cu}} = 1/2$  (Fig. 8) and confirm our previous assumption.

To estimate the magnitude of interaction we use the following equation for the magnetic susceptibility for two exchange coupled copper(II) ions [46]. The data have been fit to a model which assume the exchange Hamiltonian to be  $H = -2J\vec{S}_1 \cdot \vec{S}_2$ . The susceptibility is then predicted to be:

$$\chi_m = \frac{2N\beta^2 g^2}{3kT} \left[ 1 + \frac{1}{3} \exp(-2J/kT) \right] \quad (1)$$

and the symbols have usual meaning. Least-squares fitting of the experimental data in whole temperature range leads to  $J = -0.42$  ( $2$ )  $\text{cm}^{-1}$ ,  $g_{\text{Cu}} = 2.16(2)$ , as indicated by the solid curve in Fig. 7. The agreement factor  $R$  is equal  $9.38 \times 10^{-5}$  ( $R = \Sigma(\chi_{\text{exp}} T - \chi_{\text{calc}} T)^2 / \Sigma(\chi_{\text{exp}} T)^2$ ). The result of calculations may be indicative of

Table 2

Selected bond lengths, angles, intra- and intermolecular distances in complexes of **1**, **2** and **3** (Å, °).

Bond/distance (Å)	<b>1</b>	<b>2</b>	<b>3</b>	Angle (°)	<b>1</b>	<b>2</b>	<b>3</b>
Ln1–O1	2.441(3)	2.432(2)	2.405(4)	O1–Cu1–O2	78.6(1)	78.3(1)	78.2(2)
Ln1–O2	2.512(3)	2.507(2)	2.495(4)	O2–Cu1–N2	93.1(1)	93.1(1)	93.2(2)
Ln1–O3	2.636(3)	2.628(2)	2.596(4)	O1–Cu1–N2	158.0(2)	158.2(1)	157.3(2)
Ln1–O4	2.628(3)	2.625(2)	2.615(3)	O2–Cu1–N1	169.1(1)	169.3(1)	169.0(2)
Ln1–O6	2.587(3)	2.570(3)	2.547(5)	O1–Cu1–N1	91.6(1)	92.0(1)	91.7(2)
Cu1–O1	1.961(3)	1.961(2)	1.952(4)	N2–Cu1–N1	97.8(2)	97.6(1)	97.9(2)
Cu1–O2	1.953(3)	1.953(2)	1.948(4)	O2–Cu1–O5	91.7(1)	92.0(1)	91.4(2)
Cu1–O5	2.323(4)	2.378(3)	2.327(5)	O1–Cu1–O5	105.2(1)	104.9(1)	105.7(2)
Cu1–N1	1.971(4)	1.973(3)	1.979(5)	N2–Cu1–O5	95.3(1)	95.3(1)	95.2(2)
Cu1–N2	1.967(4)	1.963(3)	1.954(5)	N1–Cu1–O5	86.4(2)	86.0(1)	87.1(2)
Cu1–Ln1	3.618(1)	3.613(1)	3.598(1)	Cu1...Ln1...Cu1 <sup>ii</sup>	171.7(1)	172.0(1)	172.4(1)
Cu1...Cu1 <sup>i</sup>	7.218(1)	7.210(1)	7.179(1)	$\alpha$	17.4(2)	17.4(1)	16.2(2)
Cu1...Cu1 <sup>ii</sup>	7.298(1)	7.446(1)	7.252(1)	$\beta$	28.3(1)	28.4(1)	25.6(1)
Cu1...Ln1 <sup>ii</sup>	8.749(1)	8.891(1)	8.708(1)				
Ln1...Ln1 <sup>ii</sup>	10.888(1)	11.021(1)	10.872(1)				

Ln1 = Ce1 for **1**, Nd1 for **2**, Pr1 for **3**;  $\alpha$  – dihedral angle between the Cu1O1O2 and Ln1O1O2 planes;  $\beta$  – dihedral angle between two N2O2 planes; symmetry codes: <sup>i</sup>  $-x + 1, y, -z + 1/2$ ; <sup>ii</sup>  $1/2 - x, 1/2 + y, 1/2 - z$ .

**Table 3**  
Selected bond lengths, angles, intra- and intermolecular distances in complexes of **5** and **6** (Å, °).

Bond/distance (Å)	<b>5</b>	<b>6</b>	Angle (°)	<b>5</b>	<b>6</b>
Ln1–O1	2.365(2)	2.341(2)	Cu1–O1–Ln1	108.6(1)	108.7(1)
Ln1–O2	2.369(2)	2.349(2)	Cu1–O2–Ln1	107.3(1)	107.2(1)
Ln1–O3	2.524(2)	2.510(2)	O1–Ln1–O2	64.3(1)	64.7(1)
Ln1–O4	2.497(2)	2.484(2)	O1–Ln1–O3	63.9(1)	64.2(1)
Ln1–O5	2.450(3)	2.428(3)	O2–Ln1–O4	64.9(1)	65.2(1)
Ln1–O6	2.493(3)	2.473(3)	$\alpha$	2.9(1)	2.8(1)
Ln1–O8	2.345(3)	2.323(3)			
Ln1–O9	2.352(2)	2.332(2)			
Ln1–O10	2.371(2)	2.346(2)			
Cu1–N1	1.986(3)	1.986(3)			
Cu1–N2	1.960(3)	1.959(3)			
Cu1–O1	1.951(2)	1.949(2)			
Cu1–O2	1.983(2)	1.983(2)			
Cu1–O11	2.604(3)	2.600(3)			
Cu1–O14	2.552(3)	2.557(3)			
Cu1–Ln1	3.513(1)	3.495(1)			

Ln1 = Dy1 for **5**, Er1 for **6**;  $\alpha$  – dihedral angle between the Cu1O1O2 and Ln1O1O2 planes.

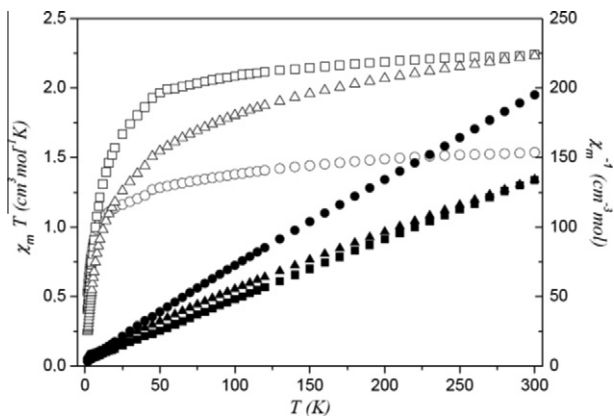


**Fig. 5.** Temperature dependence of experimental  $\chi_m T$  (○) and  $\chi_m^{-1}$  (●) vs.  $T$  for complex **1**,  $\chi_m T$  (□) and  $\chi_m^{-1}$  (■) vs.  $T$  for complex **2** and  $\chi_m T$  (△) and  $\chi_m^{-1}$  (▲) vs.  $T$  for complex **3**.

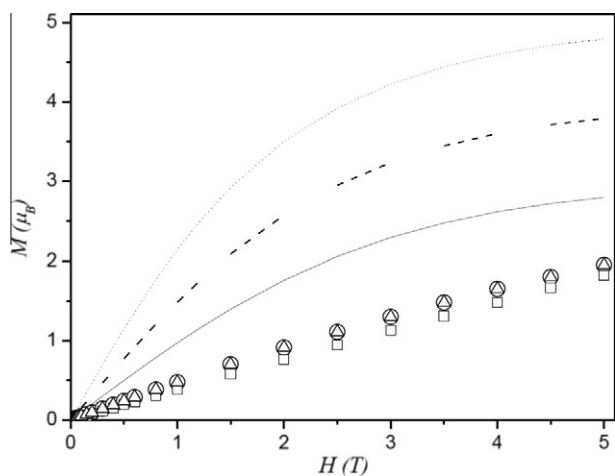


**Fig. 6.** Field dependence of the magnetization for complex **1** (○), **2** (□) and **3** (△) at 2 K. The solid line is the Brillouin function curve for a three independent  $S = 1/2$  of  $\text{Cu}^{\text{II}}\text{--Ce}^{\text{III}}\text{--Cu}^{\text{II}}$  unit; dashed line is the Brillouin function for two independent  $S = 1/2$  and one  $S = 1$  of  $\text{Cu}^{\text{II}}\text{--Pr}^{\text{III}}\text{--Cu}^{\text{II}}$  unit; dotted line is the Brillouin function for two independent  $S = 1/2$  and one  $S = 3/2$  of  $\text{Cu}^{\text{II}}\text{--Nd}^{\text{III}}\text{--Cu}^{\text{II}}$  unit.

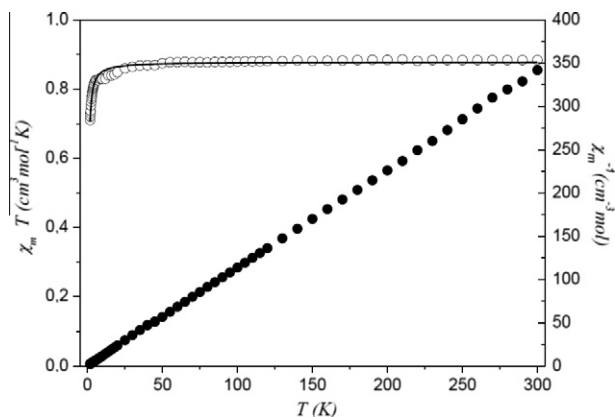


**Fig. 7.** Temperature dependence of experimental  $\chi_m T$  (○) and  $\chi_m^{-1}$  (●) vs.  $T$  for complex **4**. The solid line is the calculated curve derived from Eq. (1).

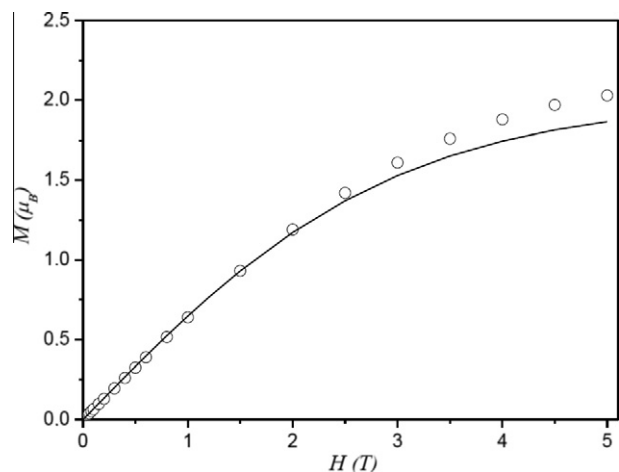


**Fig. 8.** Field dependence of the magnetization for complex **4** (○) at 2 K. The solid line is the Brillouin function curve for a two independent  $S = 1/2$  of  $\text{Cu}^{\text{II}}\text{--La}^{\text{III}}\text{--Cu}^{\text{II}}$  unit.

weak interactions between copper centers for reason of large distance  $\text{Cu} \cdots \text{Cu}$  in the trinuclear unit.

The temperature dependences of the magnetic susceptibility  $\chi_m T$  and  $\chi_m^{-1}$  of the two heterodinuclear complexes,  $\text{Cu}^{\text{II}}\text{--Dy}^{\text{III}}$  (**5**) and  $\text{Cu}^{\text{II}}\text{--Er}^{\text{III}}$  (**6**) are represented in Fig. 9. At the room temperature, the  $\chi_m T$  product is equal to  $14.92 \text{ cm}^3 \text{ mol}^{-1} \text{ K}$  for (**5**) and  $11.49 \text{ cm}^3 \text{ mol}^{-1} \text{ K}$  for **6**, which correspond the values ( $14.54$  and  $11.83 \text{ cm}^3 \text{ mol}^{-1} \text{ K}$ , respectively) expected for a pair of noninteracting  $\text{Cu}(\text{II})$  ( $S = 1/2$ ) and  $\text{Dy}(\text{III})$  ( $4f^9$ ,  $J = 15/2$ ,  $S = 5/2$ ,  $L = 5$ ,  ${}^6\text{H}_{15/2}$ ) or  $\text{Er}(\text{III})$  ( $4f^{11}$ ,  $J = 15/2$ ,  $S = 3/2$ ,  $L = 6$ ,  ${}^4\text{I}_{15/2}$ ) ions. As the temperature is lowered,  $\chi_m T$  gradually increases to reach a value of  $18.73 \text{ cm}^3 \text{ mol}^{-1} \text{ K}$  for **5** and  $12.26 \text{ cm}^3 \text{ mol}^{-1} \text{ K}$  for **6** at 10 K. The profile of the  $\chi_m T$  versus  $T$  curves are strongly suggestive of the occurrence a ferromagnetic  $\text{Cu}^{\text{II}}\text{--Ln}^{\text{III}}$  interaction in the 10–300 K temperature range. Positive value of Weiss constants could additionally confirm the ferromagnetic exchange coupling between the metal ions ( $6.9 \text{ K}$  for **5** and  $2.3 \text{ K}$  for **6**). Below 10 K, the  $\chi_m T$  values are decreased to  $11.84 \text{ cm}^3 \text{ K mol}^{-1}$  for **5** and  $9.23 \text{ cm}^3 \text{ mol}^{-1} \text{ K}$  for **6** at 1.8 K which may be attributed to zero-field splitting (ZFS) effects and/or intermolecular interactions. For the both complexes, the ground state of dysprosium(III) and erbium(III) ions have a first-order angular momentum [18,19,30], so that the magnetic properties of the  $\text{Cu}^{\text{II}}\text{--Ln}^{\text{III}}$  couples are not appropriate to a simple analysis based on a spin Hamiltonian comprising only isotropic exchange [13]. Additional difficulties may arise from the crystal field

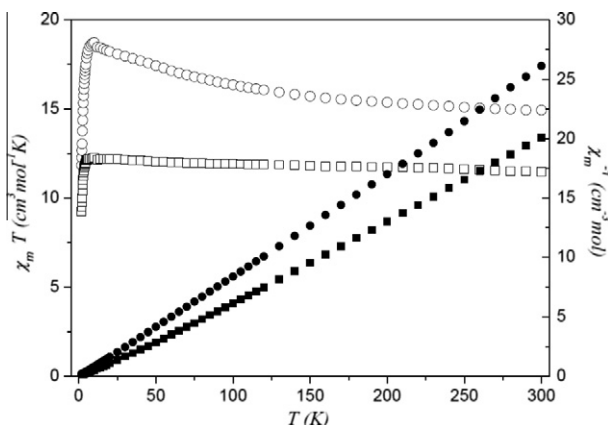


Fig. 9. Temperature dependence of experimental  $\chi_m T$  ( $\circ$ ) and  $\chi_m^{-1}$  ( $\bullet$ ) vs.  $T$  for complex **5** and  $\chi_m T$  ( $\square$ ) and  $\chi_m^{-1}$  ( $\blacksquare$ ) vs.  $T$  for complex **6**.

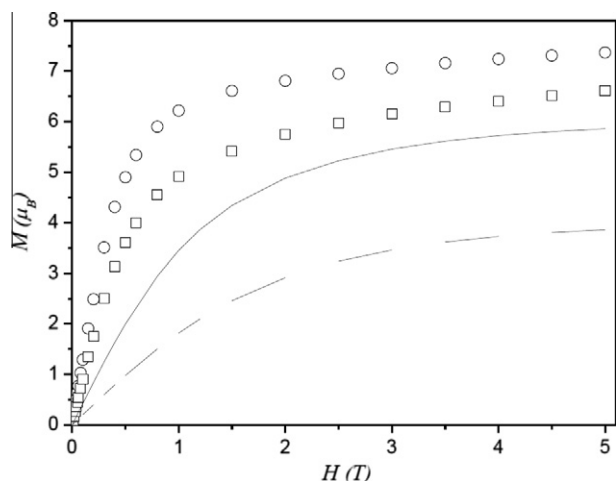


Fig. 10. Field dependence of the magnetization for complex **5** ( $\circ$ ) and **6** ( $\square$ ) at 2 K. The solid line is the Brillouin function curve for a two independent  $S = 1/2$  and  $S = 3/2$  of  $\text{Cu}^{\text{II}}-\text{Dy}^{\text{III}}$  unit; dashed line is the Brillouin function for two independent  $S = 1/2$  and  $S = 3/2$  of  $\text{Cu}^{\text{II}}-\text{Er}^{\text{III}}$  unit.

effects and the connected magnetic anisotropy [47]. Previously, we reported two similar heterodinuclear complexes,  $\text{Cu}^{\text{II}}-\text{Gd}^{\text{III}}$  and  $\text{Cu}^{\text{II}}-\text{Tb}^{\text{III}}$  [11] and magnetic investigations also reveal a ferromagnetic interaction between the Cu(II) and Ln(III) centers.

For **5** and **6** the field dependence of the magnetization  $M$  at 2 K are shown in Fig. 10. The magnetization in 5 T is equal to  $7.37 \mu_B$  for **5** and  $6.62 \mu_B$  for **6**. The  $M=f(H)$  curves are situated above the Brillouin function constructed for two isolated Ln(III) and Cu(II) systems. This fact evidences the ferromagnetic interaction between Ln(III) and Cu(II) and demonstrating that the low temperature decrease of  $\chi_m T$  is not due to ZFS effects and there exists antiferromagnetic interactions between neighboring dinuclear units.

In fact, these results are in very good agreement with the theoretical model from Kahn and co-workers [31]. Kahn et al. concluded that for the  $4f^1-4f^6$  configuration of Ln(III), angular and spin moment are antiparallel in the  $2s+1L_J$  free-ion ground state ( $J=L-S$ ). A parallel alignment of the Cu(II) and Ln(III) spin moment would lead to an antiparallel alignment of the angular moment, that is to an overall antiferromagnetic interaction, whereas for the  $4f^8-4f^{13}$  configurations ( $J=L+S$ ), a parallel alignment of the Cu(II) and Ln(III) spin moment would result in an overall ferromagnetic interaction.

## 4. Conclusion

The salen-like ligand *N,N'*-bis(5-bromo-3-methoxysalicylidene)propylene-1,3-diamine can effectively stabilize heterotri- ( $\text{Cu}-4f-\text{Cu}$ ) and heterodinuclear ( $\text{Cu}-4f$ ) complexes. The coordination compounds **1–3** are isostructural and crystallize in the monoclinic space group  $C2/c$ . Although, compound **4** gave no single crystals of quality suitable for X-ray structural analysis, we imply similar structure as in crystals of **1–3** on the basis of analogies in elemental composition and FTIR spectra. Their crystal structure is built of trinuclear dicationic units of  $[(\text{LCu}(\text{H}_2\text{O}))_2\text{Ln}(\text{NO}_3)]^{2+}$  with nitrate ions in the outer coordination sphere neutralizing the charge. The molecules have chiral two-blade propeller-like shape, however, they crystallize as racemates. In the crystal net there are channels along  $Z$  crystallographic axis filled with disordered water molecules. The heterodinuclear **5** (Dy) and **6** (Er) compounds are isostructural with other heavy lanthanide(III) complexes (Gd and Tb [11]). It is worth to study other lanthanide(III) complexes to establish the boundary radius value of Ln(III) ion for forming different types of structures. The measurement of variable-temperature magnetic susceptibility reveals antiferromagnetic interaction between spin carriers in the heterotrinuclear complexes,  $\text{Cu}^{\text{II}}-\text{Ce}^{\text{III}}-\text{Cu}^{\text{II}}$  (**1**),  $\text{Cu}^{\text{II}}-\text{Pr}^{\text{III}}-\text{Cu}^{\text{II}}$  (**2**),  $\text{Cu}^{\text{II}}-\text{Nd}^{\text{III}}-\text{Cu}^{\text{II}}$  (**3**) and ferromagnetic coupling in the heterodinuclear complexes,  $\text{Cu}^{\text{II}}-\text{Dy}^{\text{III}}$  (**5**) and  $\text{Cu}^{\text{II}}-\text{Er}^{\text{III}}$  (**6**). The magnetic data obtained for  $\text{Cu}^{\text{II}}-\text{Ln}^{\text{III}}-\text{Cu}^{\text{II}}$  (**4**) shows the weak antiferromagnetic exchange coupling between the copper ions through the diamagnetic La(III) center.

## Appendix A. Supplementary data

CCDC 832420, 858067, 832421, 858065 and 858066 contain the supplementary crystallographic data for **1**, **2**, **3**, **5** and **6**. These data can be obtained free of charge via <http://www.ccdc.cam.ac.uk/conts/retrieving.html>, or from the Cambridge Crystallographic Data Centre, 12 Union Road, Cambridge CB2 1EZ, UK; fax: (+44) 1223-336-033; or e-mail: deposit@ccdc.cam.ac.uk.

## References

- [1] P.A. Vigato, S. Tamburini, L. Bertolo, *Coord. Chem. Rev.* 251 (2007) 1311.
- [2] G. Romanowski, M. Wera, *Polyhedron* 29 (2010) 2747.
- [3] A. Jana, S. Majumder, L. Carrella, M. Nayak, T. Weyhermueller, S. Dutta, D. Schollmeyer, E. Rentschler, R. Koner, S. Mohanta, *Inorg. Chem.* 49 (2010) 9012.
- [4] L. Vaiana, M. Mato-Iglesias, D. Esteban-Gómez, C. Platas-Iglesias, A. de Blas, T. Rodríguez-Blas, *Polyhedron* 29 (2010) 2269.
- [5] T. Gao, P.F. Yan, G.M. Li, G.F. Hou, J.S. Gao, *Inorg. Chim. Acta* 361 (2008) 2051.
- [6] C. Benelli, D. Gatteschi, *Chem. Rev.* 102 (2002) 2369.
- [7] G. Marinescu, A.M. Madalan, C. Tiseanu, M. Andruh, *Polyhedron* 30 (2011) 1070.
- [8] M. Nayak, S. Hazra, P. Lemoine, R. Koner, C.R. Lucas, S. Mohanta, *Polyhedron* 27 (2008) 1201.
- [9] J.P. Costes, B. Donnadieu, R. Gheorghe, G. Novitchi, J.P. Tuchagues, L. Vendier, *Eur. J. Inorg. Chem.* (2008) 5235.
- [10] J.P. Costes, G. Novitchi, S. Shova, F. Dahan, J.P. Bruno Donnadieu, J.P. Tuchagues, *Inorg. Chem.* 43 (2004) 7792.
- [11] B. Cristóvão, J. Klak, B. Miroslaw, L. Mazur, *Inorg. Chim. Acta* (2011) 288.
- [12] X.P. Yang, R.A. Jones, W.K. Wong, V. Lynch, M.M. Oye, A.L. Holmes, *Chem. Commun.* (2006) 1836.
- [13] A. Elmali, Y. Elerman, *J. Mol. Struct.* 737 (2005) 29.
- [14] H. Wang, D. Zhang, Z.H. Ni, X. Li, L. Ti, J. Jiang, *Inorg. Chem.* 48 (2009) 5946.
- [15] J.P. Costes, F. Dahan, A. Dupuis, J.P. Laurent, *Inorg. Chem.* 35 (1996) 2400.
- [16] J.P. Costes, F. Dahan, C. R. Acad. Sci. Paris, *Chim./Chem.* 4 (2001) 97.
- [17] J.P. Costes, F. Dahan, A. Dupuis, *Inorg. Chem.* 39 (2000) 165.
- [18] R. Gheorghe, P. Cucos, M. Andruh, J.P. Costes, B. Donnadieu, S. Shova, *Chem. Eur. J.* 12 (2006) 187.
- [19] J.P. Costes, F. Dahan, A. Dupuis, J.P. Laurent, *Chem. Eur. J. Inorg. Chem.* 4 (1998) 1616.
- [20] M. Sakamoto, K. Manseki, H. Okawa, *Coord. Chem. Rev.* 219–221 (2001) 379.
- [21] M. Andruh, J.P. Costes, C. Diaz, S. Gao, *Inorg. Chem.* 48 (2009) 3342.
- [22] R. Koner, H.H. Lin, H.H. Wei, S. Mohanta, *Inorg. Chem.* 44 (2005) 3524.
- [23] R. Watanabe, K. Fujiwara, A. Okazawa, G. Tanaka, S. Yoshii, H. Nojiri, T. Ishida, *Chem. Commun.* 47 (2011) 2110.
- [24] A. Okazawa, R. Watanabe, M. Nezu, T. Shimada, S. Yoshii, H. Nojiri, T. Ishida, *Chem. Lett.* 39 (2010) 1331.
- [25] J.P. Costes, S. Shova, W. Wernsdorfer, *Dalton Trans.* (2008) 1843.

- [26] J.P. Costes, F. Dahan, A. Dupuis, *Inorg. Chem.* 39 (2000) 5994.
- [27] A.M. Atria, Y. Moreno, E. Spodine, M.T. Garland, R. Baggio, *Inorg. Chim. Acta* 335 (2002) 1.
- [28] R. Koner, G.H. Lee, Y. Wang, H.H. Wei, S. Mohanta, *Eur. J. Inorg. Chem.* (2005) 1500.
- [29] J.H. Wang, P.F. Yan, G.M. Li, J.W. Zhang, P. Chen, M. Suda, Y. Einaga, *Inorg. Chim. Acta* 363 (2010) 3706.
- [30] M.L. Kahn, C. Mathonière, O. Kahn, *Inorg. Chem.* 38 (1999) 3692.
- [31] M. Andruh, I. Ramade, E. Codjovi, O. Guillou, O. Kahn, J.C. Trombe, *J. Am. Chem. Soc.* 115 (1993) 1822.
- [32] O. Kahn, *Molecular Magnetism*, Willey-VCH, 1993.
- [33] Oxford Diffraction, Xcalibur CCD System, CrysAlis Software System, Version 1.171, Oxford Diffraction Ltd., 2009.
- [34] R.C. Clark, J.S. Reid, *Acta Crystallogr. A* 51 (1995) 887.
- [35] G.M. Sheldrick, *Acta Crystallogr. A* 64 (2008) 112.
- [36] L.J. Farrugia, *J. Appl. Crystallogr.* 32 (1999) 837.
- [37] ORTEP3 for Windows, L.J. Farrugia, *J. Appl. Crystallogr.* 30 (1997) 565.
- [38] C.F. Macrae, P.R. Edgington, P. McCabe, E. Pidcock, G.P. Shields, R. Taylor, M. Towler, J. van de Streek, *J. Appl. Crystallogr.* 39 (2006) 453.
- [39] Diamond – Crystal and Molecular Structure Visualization – Crystal Impact – K. Brandenburg and H. Putz GbR, Rathausgasse 30, D-53111 Bonn.
- [40] M.L. Kahn, T.M. Rajendiran, Y. Jeannin, C. Mathoniere, O. Kahn, *C. R. Acad. Sci. Paris, Serie IIc Chim.* 3 (2000) 131.
- [41] C. Benelli, A.J. Blake, P.E.Y. Milne, J.M. Rawson, R.E.P. Winpenny, *Chem. Eur. J.* 1 (1995) 614.
- [42] O. Guillou, R.L. Oushoorn, O. Kahn, K. Boubekeur, P. Batail, *Angew. Chem., Int. Ed. Engl.* 31 (1992) 626.
- [43] O. Guillou, P. Bergerat, O. Kahn, et al., *Inorg. Chem.* 31 (1992) 110.
- [44] O. Guillou, O. Kahn, R. Oushoorn, K. Boubekeur, P. Batail, *Inorg. Chim. Acta* 119 (1992) 198.
- [45] O. Kahn, O. Guillou, R.L. Oushoorn, et al., *New J. Chem.* 19 (1995) 655.
- [46] B. Bleaney, K.D. Bowers, *Proc. R. Soc. Lond., Ser. A* 214 (1952) 451.
- [47] E.A. Boudreaux, L.N. Mulay, *Theory and Applications of Molecular Paramagnetism*, Wiley, New York, 1976.